METHODS AND CIRCUITS FOR MEASURING CLOCK SKEW ON PROGRAMMABLE LOGIC DEVICES

Siuki Chan

FIELD OF THE INVENTION

[0001] This invention relates generally to methods and circuit configurations for measuring signal skew in programmable logic devices.

BACKGROUND

[0002] A programmable logic device (PLD) is a well-known type of digital integrated circuit that may be programmed by a user (e.g., a circuit designer) to perform specified logic functions. One type of PLD, the field-programmable gate array (FPGA), typically includes an array of configurable logic blocks (CLBs) that are programmably interconnected to each other and to programmable input/output blocks (IOBs). This collection of configurable logic is personalized by loading configuration data into internal configuration memory cells that define how the CLBs, interconnections, and IOBs are configured. For a detailed discussion of an exemplary FPGA, see U.S. Patent No. 6,144,220 entitled "FPGA Architecture Using Multiplexers that Incorporate a Logic Gate," by Steven P. Young, which is incorporated herein by reference.

[0003] Figure 1 (Prior Art) depicts a conventional FPGA 100, examples of which include the Spartan™ and Virtex™ FPGAs available from Xilinx, Inc., of San Jose, California. FPGA 100 includes an array of programmably interconnected CLBs 105. FPGA 100 additionally includes a clock distribution network 110 that can be connected to internal

or external clock sources via a global clock buffer BUFG. Many other FPGA resources are omitted from Figure 1 for brevity.

Manufacturers of PLDs, including FPGAs, would [0004] like to guarantee the highest speed performance possible without devices failing to meet the guaranteed timing specifications. PLD designers therefore measure circuit timing as accurately as possible to minimize the guard bands required to ensure correct device performance. U.S. Patent No. 6,144,262 entitled "Circuit for Measuring Signal Delays of Asynchronous Register Inputs," by Christopher Kingsley describes circuits and methods of measuring circuit timing in programmable logic devices, and is incorporated herein by reference. U.S. Patent No. 5,795,068 entitled "Method and Apparatus for Measuring Localized Temperatures and Voltages on Integrated Circuits, " by Robert O. Conn describes ring oscillator configurations on FPGAs, and is also incorporated herein by reference.

[0005] Clock distribution network 110 includes a source spine 110S that conveys clock signals to a source node 112 in the interior of FPGA 100. From there, a horizontal spine 110H conveys clock signals to a number of vertical clock spines 110V. Finally, a number of clock destination branches 110D extend to each CLB 105. Clock distribution network 110 can be programmably connected to any of CLBs 105 via programmable interconnect points. The above-cited Young patent describes exemplary programming technologies.

[0006] Clock distribution network 110 typically includes clock buffers 115 placed and sized to minimize clock skew, where skew is defined as the difference in path delays from





clock input GCLK to each of CLBs 105 and any other clock loads, such as embedded blocks of memory and IOBs.

[0007] Clock distribution network 110 is designed to minimized clock skew, and so the delays inherent in network 110 are short relative to the delays associated with other FPGA resources. The short skew is beneficial from the standpoint of performance, but renders difficult the task of accurately determining clock skew because the test circuitry normally introduces more skew than the clock network. There is therefore a need for a more accurate means of measuring clock skew on programmable logic devices.

SUMMARY

[0008] The present invention is directed to a method for accurately measuring the skew of clock distribution networks on programmable logic devices. Individual clock distribution networks are modeled using a sequence of delay-element configurations formed on the device using configurable logic. Each delay element includes a portion of the clock network for which skew is of interest, and consequently exhibits a delay that depends, in part, on the skew imposed by the portion of interest. The delay through each delay element is measured by incorporating the delay element into ring oscillators and measuring the resulting period.

[0009] The various delay-element configurations are modeled mathematically as the sum of a series of delays. The delay-element configurations are designed so their respective equations can be combined to solve for the delay contribution, or skew, of the portion of the clock network for which skew is to be measured. The delay associated



with the portion of interest can then be combined with skew measurements for other portions of the clock network to more completely describe the network.

[0010] The claims, and not this summary, define the scope of the invention.

BRIEF DESCRIPTION OF THE FIGURES

[0011] Figure 1 (Prior Art) depicts a conventional FPGA 100.

[0012] Figure 2A depicts an FPGA oscillator configuration 200.

[0013] Figure 2B depicts an FPGA oscillator configuration 250.

[0014] Figures 3A and 3B depict respective FPGA oscillator configurations 300 and 350.

[0015] Figures 4A, 4B, 4C, and 4D depict respective oscillator configurations 400, 420, 440, and 460.

[0016] Figure 5 depicts an oscillator configuration 500 implemented on an FPGA that includes one or more blocks of dedicated user memory.

DETAILED DESCRIPTION

[0017] Figures 2A-4D schematically depict FPGA configurations used in accordance with embodiments of the invention to accurately measure global clock skew for clock distribution network 110 of Figure 1. In the examples, the FPGA is a Virtex™ XCV1000 FPGA, available from Xilinx, Inc., which includes an array of 96 columns and 64 rows of CLBs, or a total of 6,144 CLBs. The number of CLBs and other FPGA resources shown in the figures is limited for brevity.

[0018] Figure 2A depicts an FPGA oscillator configuration 200 in which a CLB R24C36 (for row 24, column 36), a CLB R24C37, and a feedback circuit 205 are interconnected to form a ring oscillator. Circuit 205 and the associated connections -- made up of available FPGA resources -- connect to clock distribution network 110 via global clock buffer BUFG. The resources interconnected as shown using dashed and bold interconnect and clock lines form a ring oscillator. In the depicted embodiment, CLB R24C36 is configured to be synchronous and non-inverting, though different synchronous or asynchronous configurations might also be used.

The FPGA is programmed (i.e., configured) so the [0019] global clock buffer BUFG connects to the clock input terminal of CLB R24C36 via source spine 110S, horizontal clock spine 110H, a vertical clock spine S1 (part of a spine 110V), and one of destination branches 110D. The synchronous output terminal of CLB R24C36 is programmably connected to an input terminal of CLB R24C37 via some programmable interconnect resources depicted as net C36->C37. Finally, an output terminal of CLB R24C37 is programmably connected to the input terminal of global buffer BUFG via programmable interconnect resources 215 and 220 and circuit 205. As oscillator configuration 200 oscillates, the oscillation period T_{200} provides a measure of the speed of the interconnected components. For example, if the average period T_{200} is ten nanoseconds, then the average time required for positive- and negative-going signal transitions to traverse the components in the ring is ten nanoseconds. In the depicted embodiment, CLB R24C37 is connected in the ring via asynchronous input and output terminals, though synchronous input and output terminals



may be used in other embodiments. The above-incorporated Kingsley patent describes some oscillators for use with the present invention; other embodiment will be readily apparent to those of skill in the art.

[0020] The delay around oscillator 200 is the sum of the delays associated with horizontal spine 110H, vertical spine S1, a twelve-column-long (12C) portion of a destination branch 110D, the clock-to-out (Clk->Out) delay of CLB R24C36, the interconnect delay of net C36->C37, and the combined delays K of the delay through CLB R24C37, connections 215 and 220, circuit 205, buffer BUFG, and source spine 110S. The analysis can be simplified by assuming nearby CLBs exhibit identical clock-to-out (Clk->Out) delays. This is a reasonable assumption, particularly for identical components formed in close proximity.

[0021] Stated mathematically, the oscillation period T_{200} of oscillator configuration 200 is:

$$T_{200} = VSK + VS1 + 12C + C1k -> Out + C36 -> C37 + K$$
 (1)

[0022] where VSK is the skew between spines S1 and S2, VS1 is delay component contributed by a portion of vertical spine S1, 12C is the delay associated with a 12-column-long portion of branch 110D, Clk->Out is the clock-to-out delay of a CLB, C36->C37 is the delay encountered by signals traveling left-to-right from column 36 to column 37, and K is the delay associated with that portion of oscillator configuration 200 depicted using dashed lines.

[0023] The oscillation period T_{200} of configuration 200 is generally not, by itself, enough information to determine the delay associated with any one of the



components of the ring. The FPGA is therefore reconfigured to form one or more additional test structures.

Figure 2B depicts an FPGA configuration 250 in which a pair of CLBs R24C37 and R2438, global clock buffer BUFG, and the identical circuit 205 of Figure 2A are interconnected to form a second ring oscillator. CLB R24C37, circuit 205, clock buffer BUFG, and the dashed portion of clock distribution network 110 and interconnect resources 215 and 220 are identical to the like-identified structures of Figure 2A; consequently, the sum of the combined delay contributions of those elements, "K" in equation 1, is identical in oscillator configurations 200 and 250. The portions of the oscillators depicted as connected via solid line in the figures can be considered delay elements for which the difference in signal propagation delays provides a measure of clock skew. Including the delay elements in ring oscillators allows for accurate measures of propagation delay through the delay elements.

[0025] In Figure 2B, the FPGA is programmed so the clock input terminal of CLB R24C38 connects to the output terminal of global clock buffer BUFG via an 11-column long portion of one of destination branches 110D, vertical spine S2, and source spine 110S. The synchronous output terminal of CLB R24C38 is programmably connected to an asynchronous input terminal of CLB R24C37 via some programmable interconnect resources depicted as net C37<-C38. Finally, as in configuration 200, an output terminal of CLB R24C37 is programmably connected to the input terminal of global buffer BUFG via programmable interconnect resources 215 and 220 and circuit 205.

[0026] Stated mathematically, the oscillation period T_{250} of oscillator configuration 250 is:

$$T_{250} = VS2 + 11C + Clk -> Out + C37 <- C38 + K$$
 (2)

[0027] where VS2 is the delay of a portion of vertical spine 110V, 11C is the delay associated with an 11-columnlong portion of a branch 110D, Clk->Out is the clock-to-out delay of CLB R24C38, C37<-C38 is the delay encountered by signals traveling right-to-left from column 38 to column 37, and K is the delay associated with that portion of oscillator configuration 250 depicted using dashed lines, including the delay through CLB R24C37.

[0028] Comparing periods T_{200} and T_{250} of respective configurations 200 and 250 provides a measure of the skew VSK between verticals spines S1 and S2. Subtracting equation 2 from equation 1 gives:

$$T_{200} - T_{250} = (VSK + VS1 + 12C + Clk - > Out + C36 - > C37 + K) - (VS2 + 11C + Clk - > Out + C37 < - C38 + K)$$

$$= VSK + VS1 - VS2 + C + C36 - > C37 - C37 < - C38$$
 (3)

[0029] Delays VS1 and VS2 are from identical or nearly identical resources, and therefore can be presumed to be equal (i.e., VS1 = VS2). Thus,

$$T_{200} - T_{250} = VSK + C + C36 -> C37 - C37 <- C38$$
 (4)

[0030] Different programmable logic devices route differently. For a given PLD, the values of C36->C37 and C37<-C38 may be close enough to assume they cancel one another. Moreover, the contribution of one-column-width of

ODEILHO LOUGO



clock delay C can either be ignored or estimated by simulation. Such assumptions reduce the number of measurements used to find VSK, the skew between vertical spines S1 and S2. For example, assuming C36->C37 = C37<-C38 simplifies equation 4 to:

$$VSK = T_{200} - T_{250} - C (5)$$

[0031] Skew VSK can thus be approximated using periods T200 and T250.

[0032] It may be difficult or impossible to route some PLDs such that the left-to-right connections (e.g., C36->C37) provide the same delays as the right-to-left connections (e.g., C37<-C38). In such cases, equation 4 cannot be simplified to equation 5. The contribution of one-column-width of clock delay C might also be of Such cases may warrant additional measurements.

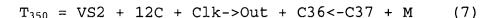
Figures 3A and 3B depict respective oscillator configurations 300 and 350, the periods of which provide additional data for finding the skew between spines S1 and S2. As with the preceding figures, the dashed and bold lines indicate which components form the oscillators. dashed lines and components are identical circuit configurations in both Figures 3A and 3B, and their equivalent delay contributions are symbolized by a constant Μ.

Using the same method described above for [0034] determining the periods associated with oscillator configurations 200 and 250, the respective periods T_{300} and T_{350} of oscillator configurations 300 and 350 are:

 $T_{300} = VSK + VS1 + 11C + Clk->Out + C35->C36 + M$ (6) and

<u>|</u>





Recalling that VS1 = VS2 and subtracting equation 7 from equation 6 gives:

$$T_{300} - T_{350} = (VS1 + VSK + 11C + C1k->Out + C35->C36 + M) - (VS2 + 12C + C1k->Out + C36<-C37 + M)$$

$$= VSK - C + C35->C36 - C36<-C37$$
 (8)

[0035] Some PLDs, including Virtex™ FPGAs, can be configured so all of the left-to-right connections are identical (e.g., C35->C36 = C36->C37) and all right-to-left connections are identical (e.g., C35<-C36 = C36<-C37). Thus configured, the contributions of like connections can be combined for simplicity. Letting DLR = delay left-to-right and DRL = delay right-to-left and adding equations 4 and 8 gives:

$$T_{200} - T_{250} + T_{300} - T_{350} = 2(VSK + DLR - DRL)$$
 (9)

or

$$VSK = (T_{200} - T_{250} + T_{300} - T_{350})/2 + DRL - DLR$$
 (10)

where VSK is the skew between vertical spines S1 and S2, the parameter of interest.

[0036] As can be seen in equation 9, the data obtained using oscillator configurations 300 and 350 cancelled the contribution of one-column-width of delay C from the resulting skew measurement, leaving skew VSK dependent only upon the measured periods and the difference in delays between the left-to-right and right-to-left connections between adjacent CLBs.

[0037] Figures 4A, 4B, 4C, and 4D depict oscillator configurations 400, 420, 440, and 460, the periods of which provide additional data for finding the difference between the left-to-right delay DLR and the right-to-left delay DRL. This difference DLR-DRL can then be used with equation 10 to calculate the skew VSK between vertical clock spines S1 and S2. As with the preceding figures, the dashed and bold lines indicated which components form the oscillators. The dashed lines and components are identical circuit configurations in each of Figures 4A-4D, and a constant N symbolizes their delay contributions.

[0038] Using the same method described above for determining the periods associated with oscillator configurations 200 and 250, the respective periods T_{400} , T_{420} , T_{440} , and T_{460} of oscillator configurations 400, 420, 440, and 460 are:

$$T_{400} = VSK + VS1 + 10C + Clk -> Out + DLR + N$$
 (11)

$$T_{420} = VSK + VS1 + 12C + Clk -> Out + DRL + N$$
 (12)

$$T_{440} = VS2 + 12C + Clk -> Out + DLR + N$$
 (13)

and

$$T_{460} = VS2 + 10C + Clk -> Out + DRL + N$$
 (14)

Subtracting equation 12 from equation 11 gives:

$$T_{400} - T_{420} = DLR - DRL - 2C$$
 (15)

Subtracting equation 14 from equation 13 gives:

$$T_{440} - T_{460} = DLR - DRL + 2C$$
 (16)

Adding equations 15 and 16 gives:

$$T_{400} - T_{420} + T_{440} - T_{460} = 2 (DLR - DRL)$$

or
 $DLR - DRL = (T_{400} - T_{420} + T_{440} - T_{460})/2$ (17)

Multiplying equation 17 by -1 gives:

$$DRL - DLR = (T_{420} - T_{400} + T_{460} - T_{440})/2$$
 (18)

[0039] Oscillator configurations 400, 420, 440, and 460 of Figures 4A-4D thus collectively provide a measure of the difference in delay between right-to-left and left-to-right programmable interconnections between adjacent CLBs. The resulting time measurement DRL - DLR can be used to solve for skew VSK using equation 10 as follows:

$$VSK = (T_{200} - T_{250} + T_{300} - T_{350})/2 + (T_{420} - T_{400} + T_{460} - T_{440})/2$$
(19)

or

$$VSK = (T_{200} - T_{250} + T_{300} - T_{350} + T_{420} - T_{400} + T_{460} - T_{440}) / 2$$
 (20)

[0040] Thus, the eight oscillator configurations depicted in Figures 2A-4D collectively provide the information required for an accurate measurement of the skew VSK between vertical clock spines S1 and S2.

[0041] Figure 5 depicts an oscillator configuration 500 implemented on an FPGA, such as a Virtex™E device, that includes one or more blocks of dedicated user memory. For a detailed description of Virtex™E FPGAs, see the Xilinx Advance Product Specification, DS022 (v1.3) February 28, 2000, pages 3-1 to 3-74, which is incorporated herein by reference.

[0042] In the FPGA of Figure 5, an embedded memory block 505 is arranged in a column extending between CLB column 36 and CLB column 37. The skew-measurement methods described above can be used for the device of Figure 5, assuming the delay contribution of left-to-right connection 510 equals



delay contribution DLR for a one-column left-to-right connection plus some delay associated with traversing memory block 505 (i.e., DLR + D_{MEM}) and the delay contribution of a right-to-left connection across memory block 510 (not shown) is delay contribution DRL for a one-column right-to-left connection plus the delay associated with traversing memory block 505 (i.e., DRL + D_{MEM}). The foregoing methods can be used to measure clock skew because the delay contribution D_{MEM} associated with memory 505 cancels in the application of the foregoing equations so equation 20 still provides a valid measure of skew VSK.

[0043] Referring back to Figure 1, the depicted FPGA includes five vertical clock spines 110V. The above-described methods can be used to find the skew between the first and second vertical clock spines, the second and third vertical clock spines, the third and fourth vertical clock spines, and the fourth and fifth vertical clock spines. The resulting collection of data can then be used to determine the skew between any two vertical clock spines.

Vertical clock spines in the depicted examples. Skew measurements between destination branches 110D may also be of interest, and can be combined with the above-described skew measurements to give a comprehensive skew analysis for an entire FPGA. Patent Application Serial No. _______ entitled "METHODS AND CIRCUITS FOR MEASURING CLOCK SKEW ON PROGRAMMABLE LOGIC DEVICES," by Siuki Chan, filed herewith [docket number X-885], describes methods of measuring skew between destination branches and is incorporated herein by reference.





[0045] FPGA components are connected in various ways: some components are directly connected, others are connected via intermediate components, such as buffers, and still others are programmably connectable, which is to say they can be programmably connected via programmable interconnect resources. In each instance, components are connected to establish some desired electrical communication between two or more circuit nodes, or terminals. Such communication may often be accomplished using a number of circuit configurations, as will be understood by those of skill in the art.

[0046] While the present invention has been described in connection with specific embodiments, variations of these embodiments will be obvious to those of ordinary skill in the art. For example, multiple embodiments of the above-described oscillator configurations can be used simultaneously on devices that include more than one signal tree for which skew measurements are of interest.

Moreover, above-described skew measurements can be done in any order, and other rows of CLBs (e.g., row 24 of Figures 2A-5) could just as easily be used to perform skew measurements. Therefore, the spirit and scope of the appended claims should not be limited to the foregoing description.